processes

MDPI

Article

The Biofungicide Activity of Some Plant Essential Oils for the Cleaner Production of Model Linen Fibers Similar to Those Used in Ancient Egyptian Mummification

Maisa M. A. Mansour [1], Mervat EL-Hefny [2,*], Mohamed Z. M. Salem [3] and Hayssam M. Ali [4,5]

1 Conservation Department, Faculty of Archaeology, Cairo University, Giza 12613, Egypt; maisamansour_40@yahoo.com
2 Department of Floriculture, Ornamental Horticulture and Garden Design, Faculty of Agriculture (El-Shatby), Alexandria University, Alexandria 21545, Egypt
3 Forestry and Wood Technology Department, Faculty of Agriculture (EL-Shatby), Alexandria University, Alexandria 21545, Egypt; zidan_forest@yahoo.com
4 Botany and Microbiology Department, College of Science, King Saud University, P.O. Box 2455, Riyadh 11451, Saudi Arabia; hayhassan@ksu.edu.sa
5 Timber Trees Research Department, Sabahia Horticulture Research Station, Horticulture Research Institute, Agriculture Research Center, Alexandria 21526, Egypt
* Correspondence: mervat.mohamed@alexu.edu.eg

Received: 11 December 2019; Accepted: 3 January 2020; Published: 7 January 2020

Abstract: In this work, the essential oils (EOs) from *Eriocephalus africanus* leaf, *Vitex agnus-castus* leaf and fruit, *Cymbopogon citratus* leaf, and *Rosmarinus officinalis* leaf were used as antifungal agents against isolated *Aspergillus flavus*, *Cladosporium cladosporioides*, and *Penicillium chrysogenum* from an ancient Egyptian child's mummy. The isolated fungi were used to colonize the samples of linen fibers. The best oil was used as a novel natural product for the cleaner production of model linen fibers similar to those used in ancient Egyptian mummification. Standard and original linen fibers were compared with the infected Linen samples using Fourier transform infrared (FTIR) and X-ray diffraction (XRD) analyses. The FTIR revealed the changes in the molecular structure of the cellulose, hemicellulose, and lignin of the infected linen fibers. The cellulose crystallinity indices decreased to 64.61%, 52.69%, and 54.63% in the linen inoculated with *A. flavus*, *C. cladosporioides*, and *P. chrysogenum* compared to the control sample (72.08%), thereby affecting the chemical properties of the cellulose. The mycelia inhibition percentages of the three fungi reached 100% after the leaf EO from *V. agnus-castus* was applied, followed by *C. citratus*. The *V. agnus-castus* leaf EO applied at contraptions of 250, 500, 50, 1000, and 2000 µL/mL showed 100% inhibition for *A. flavus* and *P. chrysogenum* and reached 100% against *C. cladosporioides* at concentrations of 500, 750, 1000, and 2000 µL/mL. *C. citratus* leaf essential oil applied at concentrations of 500, 750, 1000, and 2000 µL/mL showed 100% inhibition to the growth of *A. flavus* and *C. cladosporioides* and reached 100% inhibition against the growth of *P. chrysogenum* at concentrations of 750, 1000 and 2000 µL/mL. This inhibition could be related to the main compounds of caryophyllene (23.13%), eucalyptol (20.59%), sabinene (β-thujene) (12.2%), γ-elemene (9%), and β-farnesene (6.14%) identified in *V. agnus-castus* leaf EO or due to the main compounds of β-citral (43.63%) and geranial (41.51%), as identified in the leaf EO of *C. citratus* by GC/MS. The morphological changes in the hyphae of the fungi were observed via SEM examination, where *V. agnus-castus* leaf EO, the best active oil, showed potent inhibition to fungi grown on the model linen fiber. In this way, the morphology and the structure of the hyphae were effectively changed. Our findings prove that the designed model linen fiber treated with *V. agnus-castus* leaf EO is able to preserve wrapping fibres and represents a novel natural alternative for effective fungicidal treatment.

Keywords: essential oil; biofungicide activity; model linen fiber; ancient Egyptian mummification; SEM examination

1. Introduction

Plants are rich in phenols, oxides, esters, monoterpenoids, and other compounds that have a broad spectrum of use for their potential antimicrobial activities [1–11]. Indeed, essential oils (EOs) have some important uses as antifungal agents, with many applications [2,4,5,12]. The EO obtained from the fresh leaves of *Cympobogon citratus* (Lemongrass) contain geranial (α-citral) and neral (β-citral) [13,14]. While in the other study, citronellal, limonene, β-myrcene, and geraniol were found to be the main compounds [15]. Plant EOs have bactericidal and fungicidal effects against Gram-positive and -negative bacteria, molds, and yeasts [16,17].

The major chemical constituents of the EO from *Rosmarinus officinalis* (Rosemary) are camphor, 1,8-cineol, camphene, verbenone, and pinene [18,19], which have antifungal activity against *Penicillium digitatum* [20] and also act as antibacterial and antifungal agents against some spoilage organisms (Rezzoug et al., 2005).

The abundant compounds of the EOs obtained from *Vitex agnus-castus* L. fruits and leaves were sabinene, 1,8-cineole, and α-pinene, which have potential antimicrobial activities [21]. Oil from the leaves of *V. agenus-castus* showed the presence of eucalyptol, (E)-β-caryophyllene, and β-sitosterol as the main compounds [9].

Artemisia ketone, intermedeol, and γ-eudesmol were the main compounds in the EO of *Eriocephalus africanus* L. [22], while Artemisia ketone and ledol were the main compounds in the essential oil from the leaves of *E. africanus* grown in Egypt [5], with observable antibacterial activity. The organic solvent extracts (ethanol, methanol, and chloroform) of *E. africanus* exhibited antifungal activities against *Candida albicans* [23].

The cultural heritage deterioration caused by the activity of fungi such as *Aspergillus*, *Penicillium*, *Alternaria*, *Cladosporium*, *Aureobasidium*, *Geotrichum*, *Mucor*, *Pullularia*, and *Rhizopus* has become a global problem [24–26]. These deteriorating fungi can colonize archaeological objects, such as mummies, faiences, paintings, clothing, books, and manuscripts, thereby changing their structures through the chemical and physical processes of enzymatic degradation, the production of acids, and mechanical attacks [7,27,28]. Additionally, the biodeterioration caused by fungi results in discoloration, crushing, spots, cracking, loss of strength, smell, and loss of material [28,29].

Historical textile materials, when exposed to high humidity, can be easily decayed by cellulolytic fungi, where their mycelia penetrate into cellulosic material resulting in a loss of fiber strength [30–32]. At low temperatures and relative humidity (RH), some fungal contaminations by *P. chrysogenum* and *C. cladosporioides* can be found as white mycelium spots on both leathers and textiles [28,33,34]. Saprophytic fungi, including *Penicillium*, *Alternaria*, *A. fumigatus*, *A. nidulans*, *Rhizopus* and *Chrysosporium*, have been isolated from a mummy from the archaeological museum in Zagreb [35]. Recently, *A. flavus*, *C. cladosporioides*, and *P. chrysogenum* were isolated from a child's mummy discovered in Egypt [36].

Therefore, the present study aimed firstly to evaluate the antifungal activity of five natural EOs against the growth of three fungi isolated from an Egyptian child's mummy and secondly to identify the best active oils to treat the model linen fibers similar to those used in Egyptian mummification.

Changes in the functional chemical groups and cellulose crystallinity of the linen fibers affected by inoculation with the three fungi were measured by FTIR and XRD, while SEM examination was used to show the deterioration in the linen fibers and the inhibition of fungal growth after treating the model fibers with the best active EO.

2. Materials and Methods

2.1. Isolated Fungi from the Ancient Egyptian Child Mummy and Colonization Test

We used the following three fungi, *Aspergillus flavus*, *Cladosporium cladosporioides*, and *Penicillium chrysogenum* (under the accession numbers LC325160, LC325159, and LC325162, respectively), previously isolated from the mummy of a child aged 6 to 8 years and identified using internal transcribed spacer (ITS) sequencing [36].

For the colonization test, standard linen samples cut into 2 × 2 cm squares using a scalpel and saturated with liquid media and maintained on a malt extract agar (MEA) (Sigma–Aldrich, Darmstadt, Germany) with 5% NaCl (Sigma–Aldrich, Darmstadt, Germany) were inoculated with a spore suspension from each of the three fungi, according to the recommendations of Miller et al. [37], Mansour [36], and Mohamed et al. [7].

2.2. FTIR Analysis of the Standard, Original, and Infected Linen Samples

Three months after the inoculation of the linen fibers with each of the three fungi, an Fourier transform infrared (FTIR) spectrometer (Model 6100 Jasco, Tokyo, Japan) was used to analyze the samples. This analytical technique was performed on both the used linen fiber (2 cm × 2 cm) and on a linen sample from the original mummy (small fragments).

2.3. X-ray Diffraction Analysis (XRD) for the Crystallinity Index

The band positions of the crystalline and amorphous cellulose forms of the studied control and the samples colonized with *A. flavus*, *C. cladosporioides*, and *P. chrysogenum* were measured using a Philips Analytical X-ray (Philips–Eindhoven—The Netherlands) by means of Match 3 + PDF-4 2015 software program (Kreuzherrenstr, Bonn, Germany) diffractometer type: PW 1840, with a Cu tube anode, a generator tension of 40 kV, and a generator current of 25 mA). The crystallinity index (CI) was measured according to Segal et al. [38] with the following formula:

$$CI \equiv \frac{I_{002} - I_{am}}{I_{002}} \times 100 \quad (1)$$

where I_{002} is the diffraction intensity at the 002 peak position ($2\theta \approx 22.5°$) and I_{am} at $2\theta = 18°$ (angle of amorphous cellulose).

2.4. Antifungal Activity of Essential Oils

2.4.1. Plant Material and Essential Oil Extraction

The *Eriocephalus africanus* leaf, *Vitex agnus-castus* (leaf and fruit), *Cymbopogon citratus* leaf, and *Rosmarinus officinalis* leaf, were collected in 2017 from the nursery of the Department of Floriculture, Ornamental Plants and Garden Design, Faculty of Agriculture, Alexandria University, Alexandria, Egypt. The plants were identified and authenticated by the co-author Dr. Mervat El-Hefny. The essential oils (EOs) were extracted via the water distillation method using a proper essential oil trap (Clevenger's apparatus) [39]. The EOs were kept dry in sealed Eppendorf tubes at 4 °C to wait for the chemical analysis.

2.4.2. GC/MS Analysis of the EOs

A Trace GC Ultra/Mass spectrophotometer ISQ (Thermo Scientific) instrument equipped with a flame ionization detector and a DB-5 narrow bore column (Agilent, Palo Alto, CA, USA) was used. The temperature program of the column oven and the other specifications of the operating system can be found in a previously published work [40]. Briefly, The GC–MS was equipped with a ZB-5MS Zebron capillary column (length 30 m × 0.25 mm ID, 0.25 µm film thickness; Agilent, Palo Alto, CA,

USA). Helium, the carrier gas, with an average velocity of 39 cm/s, was used. Firstly, the temperature of the oven was held at 45 °C (2 min); then, the temperature was increased from 45 to 165 °C at 4 °C/min and 165–280 °C at 15 °C/min. the mass spectra were measured and collected under electron impact ionization at 70 electron volts and scanned from *m/z* 50–500 at five scans/second. The identification of the chemical compositions was performed based on an MS library search [41] and confirmed by measuring the Standard and Reverse Standard Indices [7,9,42,43].

2.4.3. Preparation of Oil Concentrations and Antifungal Activity

Firstly, the stock solution was 20 mL, wherein the oil amount was diluted in 10% dimethyl sulfoxide (2 mL Dimethyl sulfoxide (DMSO) diluted in 18 mL sterilized distilled water) (Sigma–Aldrich, Darmstadt, Germany). EOs were prepared at concentrations of 62, 125, 250, 500, 1000, and 2000 µL/mL by dissolving the EO in DMSO 10%, and a few drops of Tween-80 detergent were added to each EO concentration to emulsify the carrier oils in water. The inhibitory effects of the tested EOs on the linear growth of three fungi (*Aspergillus flavus*, *Cladosporium cladosporioides*, and *Penicillium chrysogenum*) were estimated. The measurement was performed in triplicate [1,44,45]. The mycelial growth inhibition (%) was calculated according to the following equation:

$$MGI\% = \frac{A_c - A_t}{A_c} \times 100 \quad (2)$$

where the *MGI* is mycelia growth inhibition, and A_C and A_t are the average diameters of the fungal colonies of the control (10% DMSO + few drops of Tween-80) and the treatment, respectively.

2.5. Model Linen of Mummification

Firstly, the linen samples were vapour treated with concentrated EO prepared at 0 (control), 125, 250, 500, 750, 1000, and 2000 µL/mL using the evaporation method [44,46,47] with minor modification. Linen samples were placed in petri dishes containing eight layers of Wattman No. 1 filter papers (Loba Chemie Pvt. Ltd., laboratory reagents & fine chemicals, Mumbai, India) overlaid by a polyethylene spacer mesh (Hebei Hightop Metal Mesh Co., Ltd., China). Dishes were autoclaved at 121 °C for 20 min and then left to cool. Each concentration of the EO was impregnated over the filter papers and kept for 48 h. This period allow the EO (fumigant) to evaporate and subsequently become absorbed by the linen samples.

A linen piece 15 cm long and 3 cm wide layer was fumigated with the best active concentrated EO resulting from the antifungal bioassay test. The sample model of the mummy was then produced and wrapped using three layers of linen pieces 15 cm long and 3 cm wide in the form of a roll and put in the Petri dish (15 cm) (Figure 1). The linen layers with infected each fungus were put between the treated linen layers with the best active EOs and the linen layers without any treatment in the form of a wide roll. Similarly, the fumigated linen pieces (2 × 2 cm) with different concentrations of the best EO were incubated in Petri dishes and inoculated with the spores of each fungus.

2.6. Scanning Electron Microscope (SEM) Examination of Inoculated Linen with Fungi

SEM analysis was used to examine the linen inoculated with the three fungi. The SEM model was a FEI Quanta 200 SEM FEG (FEI Company, Eindhoven, The Netherlands), which was used to study changes in the surface morphology and colonization of the fungi in both the inoculated and non-inoculated linen samples.

2.7. Statistical Analysis

The mycelial growth inhibition (%) of the fungi, as affected by the five EOs with 6 concentrations, was analyzed using a two-way ANOVA, while the mycelial growth inhibition (%) resulting from the best EO applied to the model mummification linen fiber was analyzed using a one-way ANOVA.

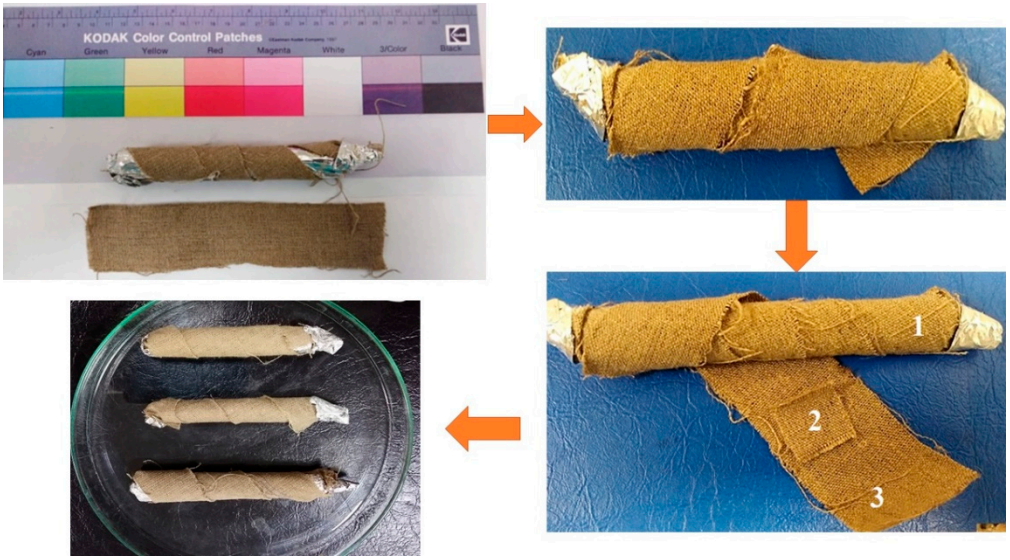

Figure 1. Model of the linen mummification and the application of oil: **1**—Linen without any treatment; **2**—linen infected by fungi; **3**—linen treated by oil.

3. Results and Discussion

3.1. FTIR Analysis of the Linen

The changes in the wavenumbers of the functional groups of the main chemical structures of the linen fibers (standard, original, and infected with fungi) are shown in Figure 2a–c. The fungal spores possess a high absorption ability in the short-wavelength spectral region (1533 cm^{-1}) due to chitin in the cell wall, as well as the high content of proteins [48]. Moreover, dramatic decreases of the band to a maximum at 1500 cm^{-1} were found, indicating a typical lignin [49]. Fungi have high absorption rate in the long-wavelength spectral region (1500–500 cm^{-1}) due to the high content of carbohydrates [50].

Due to their chemical composition (especially cellulose), historical textile materials can easily decay via *P. chrysogenum* and *C. cladosporioides* when exposed to high humidity [28,32,34]. The mycelia of cellulolytic fungi lead to the loss of fibre strength as the fungi penetrate the cellulosic materials [30,31].

The assignment of OH stretching appeared at 3300–3400 cm^{-1}, which is characteristic of OH stretching in alcohols and phenols of cellulose, lignin, or hemicellulose [11,44,51–55]. The band at 3423 cm^{-1} (–OH groups bending) in the spectrum of decayed and original samples became wider than the standard linen spectrum, and its peak shifted to a high wave, wherein hydroxyl groups on the backbone of the hemicelluloses were found.

Changes in the wavelengths at 1424 cm^{-1} and 1512 cm^{-1} confirmed the ability of fungi to decompose the lignin [55,56]. The bands' relative intensities of absorption at 1510–1267 cm^{-1} increased significantly. The lower absorption peaks of the lignin [57] occurred under hydrolysis, oxidation, and the breaking of intermolecular bonds, which were caused by fungi. It was reported that the FTIR technique might be applied to detect mound fungi growth on materials [58]. This means that the primary functional groups that reoccurred in the infected linen and the original sample were attacked by microorganisms. The crystallinity degree of native cellulose is between 60% and 90% [59,60]. Furthermore, the cellulose fibers collapsed, which means that the samples decayed [61].

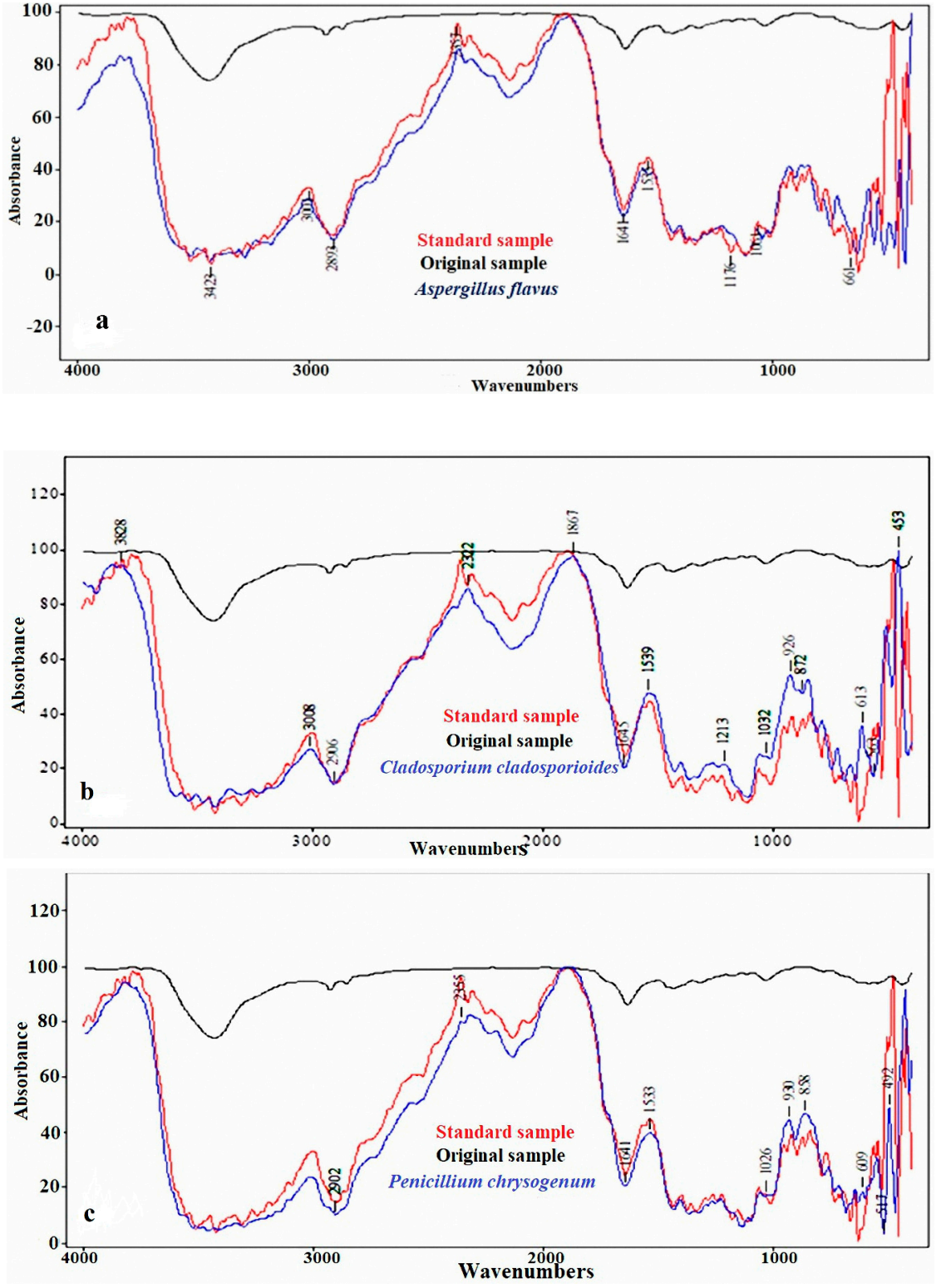

Figure 2. Fourier transform infrared (FTIR) spectra of linen fibres as affected by inoculation with (**a**) *Aspergillus flavus*, (**b**) *Cladosporium cladosporioides*, and (**c**) *Penicillium chrysogenum*.

3.2. Cellulose Crystallinity of Linen Fibers

The results of the XRD (Figure 3) showed that there are noticeable differences in the amorphous areas in the linen affected by the three molds compared to the control (Cellulose Crystallinity = 72%), as shown in Figure 3a. This indicated that fungal degradation may change the d-spacing of the

crystalline area of the cellulose and cause a slight shift to a higher theta degree of the band positions. Large decreases of 64.61%, 52.69%, and 54.63% in the crystallinity indices of the cellulose crystallinity of the linen inoculated with *A. flavus* (Figure 3b), *C. cladosporioides* (Figure 3c), and *P. chrysogenum* (Figure 3d) were found compared to the control sample (72.08%), which indicates that a change has occurred in the chemical properties of the cellulose.

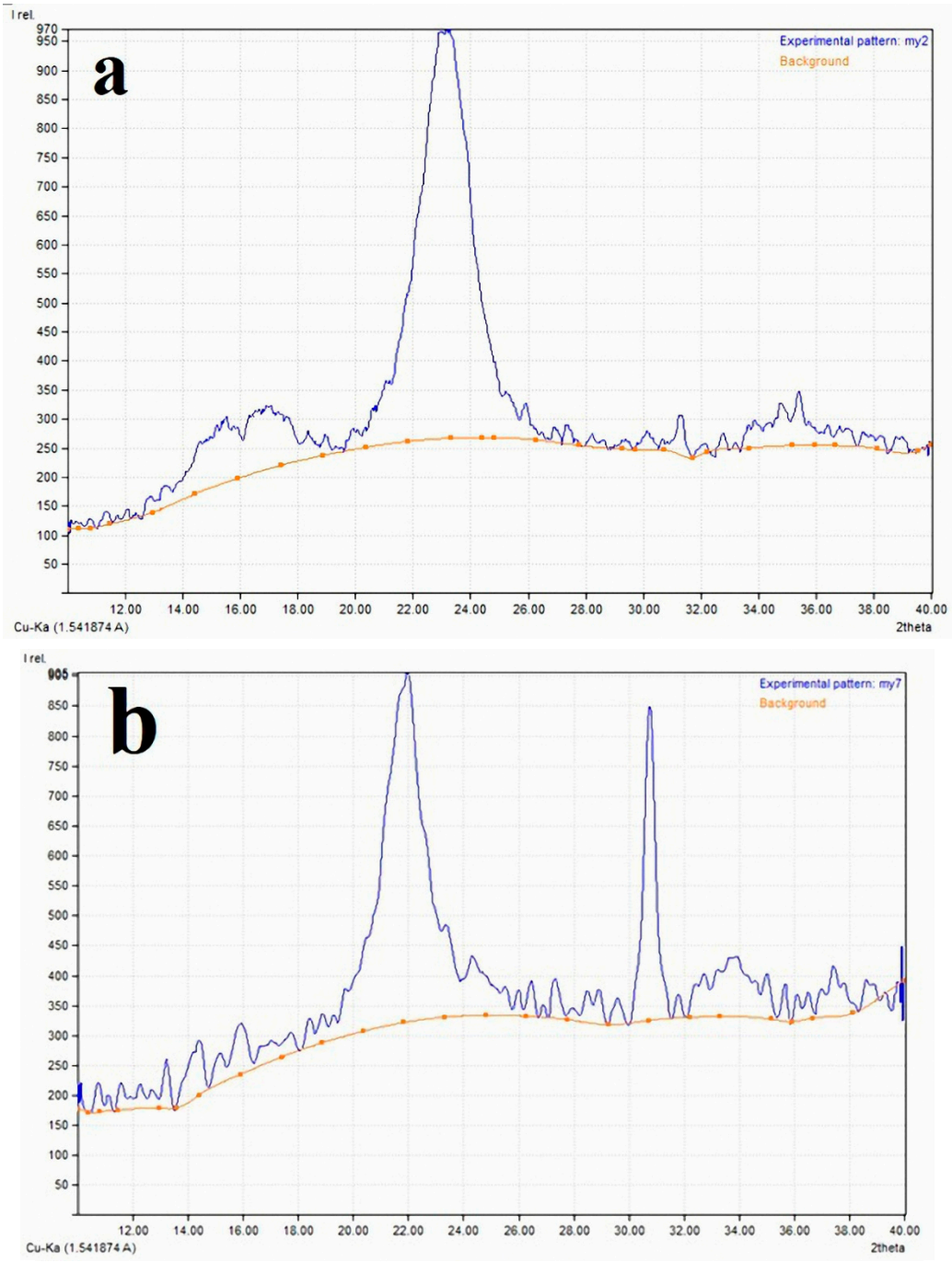

Figure 3. *Cont.*

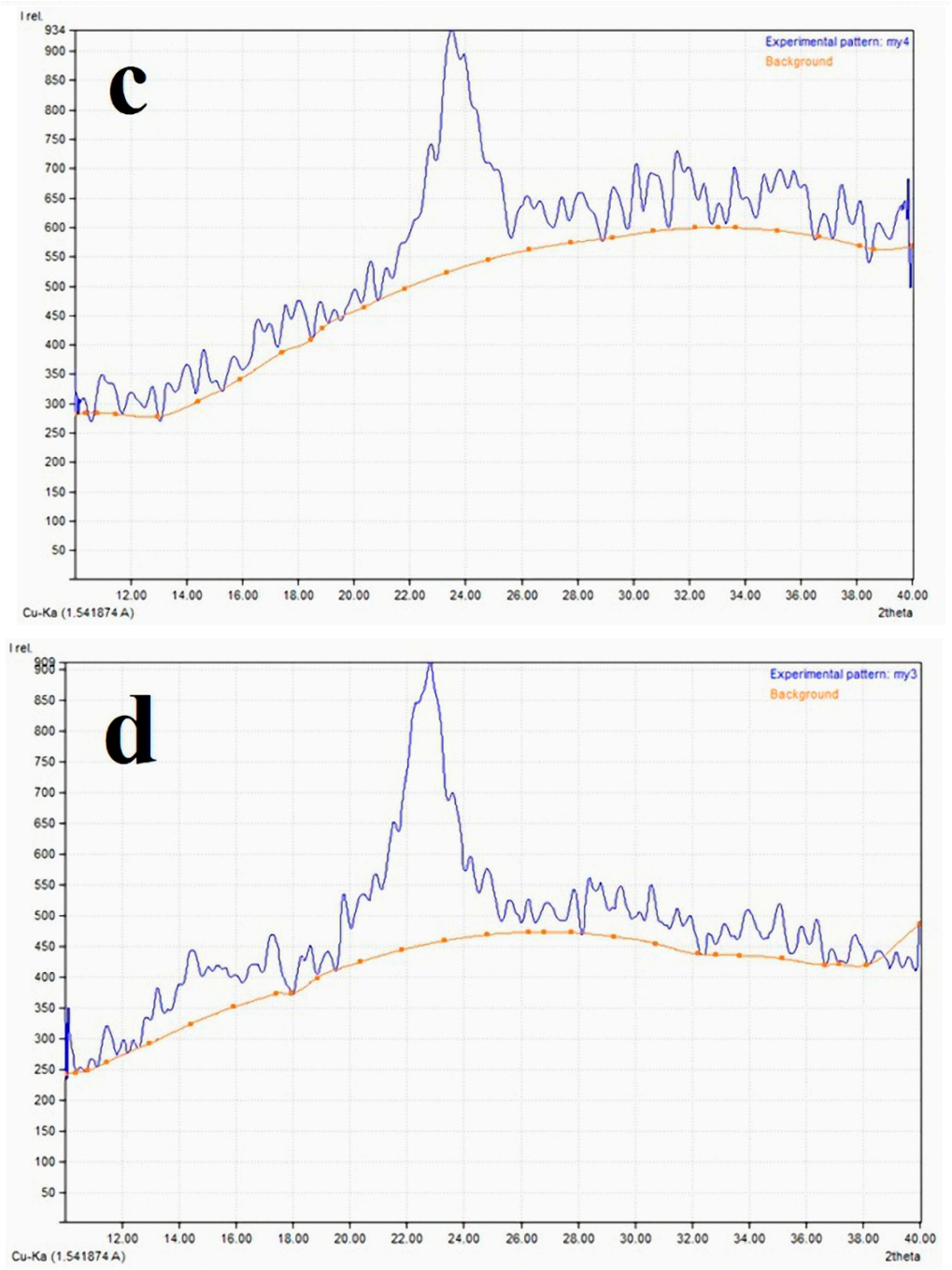

Figure 3. X-ray Diffraction Analysis (XRD) patterns for measuring the crystallinity index of the linen cellulose; (**a**) control; (**b**) linen inoculated with *A. flavus*; (**c**) linen inoculated with *C. cladosporioides*; (**d**) linen inoculated with *P. chrysogenum*.

3.3. Antifungal Activity of the EOs

The antifungal activities of the EOs of *E. africanus* leaf, *V. agnus-castus* leaf and fruit, *C. citratus* leaf, and *R. officinalis* leaf are presented in Table 1. The results of the mycelial inhibition percentages show that the leaf EO from *V. agnus-castus* possessed the best activities against the growth of *A. flavus*, *C. cladosporioides*, and *P. chrysogenum*, as most of the studied EO concentrations showed a 100% inhibition of fungal mycelial growth, followed by *C. citratus* EO.

Table 1. The effects of essential oil (EO) concentrations on the inhibition of the fungal mycelia (%) of *A. flavus*, *Cladosporium cladosporioides*, and *P. chrysogenum*.

Oil	Concentration µL/mL	Inhibition of Fungal Mycelial (%)		
		A. flavus	***C. cladosporioides***	***P. chrysogenum***
E. africanus leaves	0 (control)	0.00	0.00	0.00
	125	0.00	7.04 ± 0.64	18.14 ± 0.64
	250	37.41 ± 0.64	62.59 ± 0.64	46.29 ± 0.64
	500	61.85 ± 0.64	65.18 ± 0.64	58.52 ± 0.64
	750	68.88 ± 1.11	100 ± 0.00	75.92 ± 1.69
	1000	80.37 ± 0.64	100 ± 0.00	80.74 ± 0.64
	2000	87.77 ± 1.11	100 ± 0.00	100 ± 0.00
V. agnus-castus leaves	0 (control)	0.00	0.00	0.00
	125	76.29 ± 0.64	40 ± 1.11	51.85 ± 0.64
	250	100 ± 0.00	71.48 ± 0.64	100 ± 0.00
	500	100 ± 0.00	100 ± 0.00	100 ± 0.00
	750	100 ± 0.00	100 ± 0.00	100 ± 0.00
	1000	100 ± 0.00	100 ± 0.00	100 ± 0.00
	2000	100 ± 0.00	100 ± 0.00	1000.00
C. citratus leaves	0 (control)	0.00	0.00	0.00
	125	8.15 ± 0.64	9.63 ± 6.41	2.59 ± 0.64
	250	49.26 ± 0.64	74.07 ± 0.64	19.63 ± 0.64
	500	100 ± 0.00	100 ± 0.00	54.81 ± 0.64
	750	100 ± 0.00	100 ± 0.00	100 ± 0.00
	1000	100 ± 0.00	100 ± 0.00	100 ± 0.00
	2000	100 ± 0.00	100 ± 0.00	100 ± 0.00
R. officinalis leaves	0 (control)	0.00	0.00	0.00
	125	3.71 ± 0.64	8.88 ± 1.11	5.18 ± 7.14
	250	42.59 ± 1.69	15.92 ± 6.41	18.14 ± 6.41
	500	58.88 ± 1.11	18.88 ± 1.11	51.48 ± 0.64
	750	74.44 ± 1.11	20.74 ± 6.41	69.63 ± 6.41
	1000	88.51 ± 0.64	41.48 ± 0.64	88.51 ± 0.64
	2000	100 ± 0.00	100 ± 0.00	100 ± 0.00
V. agnus-cactus fruits	0 (control)	0.00	0.00	0.00
	125	6.66 ± 1.11	13.33 ± 11.11	0.37 ± 0.64
	250	48.52 ± 0.64	18.52 ± 0.64	16.29 ± 0.64
	500	63.71 ± 0.64	67.77 ± 1.11	47.41 ± 0.64
	750	76.66 ± 1.11	100 ± 0.00	70.37 ± 0.64
	1000	80.74 ± 0.64	100 ± 0.00	88.15 ± 1.28
	2000	100 ± 0.00	100 ± 0.00	100 ± 0.00
p-value		<0.0001	<0.0001	<0.0001

3.4. Chemical Composition of the EOs

The phytochemical constituents of *Eriocephalus africanus* leaf EO can be found in our previously published work [5]. The phytochemical constituents of *Cympobogon citratus* EO presented in Table 2 show the main abundant compounds of *β*-citral (43.63%), geranial (*α*-citral or citral A) (41.51%), *β*-myrcene (12.37%), 1,3-diolein (1.57%), and 9-octadecenoic acid (0.92%). The EO of lemongrass contains mainly citral [15] and citronellal, limonene, and geraniol [12,15].

Table 3 shows the chemical constituents of the EO from *Rosmarinus officinalis*, where the main compounds were eucalyptol (30.75%), *α*-pinene (20.41%), camphor (18.15%), borneol (5.94%), ethyl iso-allocholate (6.77%), limonene (2.72%), linalool (2.74%), and camphene (2.59%). The main chemical compounds in the EO of *R. officinalis* grown in Pakistan were 1,8-cineol, camphor, *α*-pinene, limonene, camphene, and linalool [62], while cineole, camphor, and *α*-pinene were the main compounds in Brazilian plants [63]. In Tunisian *R. officinalis*, the EOs were 1.8-cineole and camphor [64]. Camphor

(5–31%), 1,8-cineol (15–55%), camphene (2.5–12.0%), verbenone (2.2–11.1%), and pinene (9–26%) were found to be the major compounds in the EO of *R. officinalis* [18,19].

Table 2. Chemical composition of the EO from lemongrass leaves.

Compound Name	R.T. (min)	Area %	Molecular Formula	Molecular Weight	Standard Index	Reverse Standard Index
β-Myrcene	8.36	12.37	$C_{10}H_{16}$	136	955	951
β-Citral	18.4	43.63	$C_{10}H_{16}O$	152	934	934
geranial (e-citral)	19.41	41.51	$C_{10}H_{16}O$	152	926	926
9-octadecenoic acid	31.08	0.92	$C_{18}H_{34}O_2$	282	832	795
1,3-Diolein	32.82	1.57	$C_{39}H_{72}O_5$	620	794	758

R.T.: Retention time.

Table 3. Chemical composition of the EO from *R. officinalis.*

Compound Name	R.T. (min)	Area %	Molecular Formula	Molecular Weight	Standard Index	Reverse Standard Index
α-Pinene	6.99	20.41	$C_{10}H_{16}$	136	957	956
Camphene	7.7	2.59	$C_{10}H_{16}$	136	961	938
Limonene	10.09	2.72	$C_{10}H_{16}$	136	928	924
Eucalyptol	10.46	30.75	$C_{10}H_{18}O$	154	950	947
Linalool	12.86	2.74	$C_{10}H_{18}O$	154	951	938
Camphor	15.9	18.15	$C_{10}H_{16}O$	152	954	952
Borneol	16.17	5.94	$C_{10}H_{18}O$	154	911	907
Verbenone (2-Pinen-4-one)	18.41	2.29	$C_{10}H_{14}O$	150	929	916
Ethyl iso-allocholate	32.53	6.77	$C_{26}H_{44}O_5$	436	822	801

R.T.: Retention time.

Table 4 shows the chemical constituents of EO from *Vitex agnus-castus* leaves, where the main compounds are caryophyllene (23.13%), eucalyptol (20.59%), sabinene (*β*-thujene) (12.2%), *γ*-elemene (9%), *β*-farnesene (6.14%), caryophyllene oxide (4.06%), 2-methylenecholestan-3-ol (3.35%), and 1-heptatriacotanol (2.77%). Table 5 presents the chemical constituents of *V. agnus-castus* fruit EO, where the main compounds are *γ*-elemene (41.59%), geranyllinalool (17.98%), eucalyptol (16.65%), nerolidyl acetate (11.63%), *cis*-caryophyllene (3.73%), *α*-pinene (2.58%), caryophyllene oxide (2.55%), and nerolidol (1.16%). The main chemical compounds identified in the EO of *V. agnus-castus* with strong antimicrobial activities were mostly 1,8-cineole or eucalyptol, sabinene, (*E*)-*β*-farnesene, (*E*)-caryophyllene, and *α*-terpinyl acetate [9,21,65–67]. Further, 1,8-cineole has been proven to have good antifungal activity against *Aspergillus* apple rot [21]. *V. agnus-castus* oil contains the main compounds of 1,8-cineole (eucalyptol) and 8-caryophyllene, which significantly inhibited the growth of *F. oxysporum*, *R. solani*, *Sclerotinia sclerotiorum*, and *Verticillium dahlia* [68]. *Melia azedarach* wood-treated with the *n*-hexane oil of *V. agenus-castus* leaves at a 1%, 2%, or 3% concentration showed good antifungal activity against *F. culmorum*, *Rhizoctonia solani*, and *P. chrysogenum* [9], where the main compounds were eucalyptol (22.1%), (E)-β-caryophyllene (18.3%), and β-sitosterol (12.4%). The leaf EO of *V. agnus-castus* showed potent antimicrobial activity against the growth of bacteria (*Agrobacterium tumefaciens* and *Erwinia carotovora* var. carotovora) and fungi (*Alternaria alternata*, *Botrytis cinerea*, *F. oxysporum*, and *F. solani*) [69].

Table 4. Chemical composition of the essential oil from *Vitex agnus-castus* leaves.

Compound Name	R.T. (min)	Area %	Molecular Formula	Molecular Weight	Standard Index	Reverse Standard Index
α-Thujene	6.7	0.21	$C_{10}H_{16}$	136	948	912
α-Pinene	7	0.47	$C_{10}H_{16}$	136	958	950
Sabinene (β-Thujene)	8.39	12.2	$C_{10}H_{16}$	136	970	962
β-Pinene	8.63	0.56	$C_{10}H_{17}$	136	949	946
1-Octen-3-ol	9.2	0.69	$C_8H_{16}O$	128	945	931
Terpinolene	9.72	0.22	$C_{10}H_{16}$	136	932	881
Eucalyptol	10.68	20.59	$C_{10}H_{18}O$	154	950	950
γ-Terpinene	11.19	0.46	$C_{10}H_{16}$	136	136	896
Linalool	12.88	0.34	$C_{10}H_{18}O$	154	946	932
Terpinen-4-ol	16.11	2	$C_{10}H_{18}O$	154	930	930
α-Terpineol	16.84	1.67	$C_{10}H_{18}O$	154	941	938
Linalyl acetate	17.24	0.31	$C_{12}H_{20}O_2$	196	896	889
(−)-α-Gurjunene	21.61	0.62	$C_{15}H_{24}$	204	930	915
Caryophyllene	22.42	23.13	$C_{15}H_{24}$	204	960	960
β-Farnesene	22.73	6.14	$C_{15}H_{24}$	204	943	941
(+)-Aromadendrene	23.66	3.26	$C_{15}H_{24}$	204	930	913
γ-Elemene	24.91	9	$C_{15}H_{25}$	204	927	900
Viridiflorol	27.02	0.33	$C_{15}H_{26}O$	222	872	812
(−)-Spathulenol	27.58	1.79	$C_{15}H_{24}O$	220	922	891
Caryophyllene oxide	27.65	4.06	$C_{15}H_{24}O$	220	901	869
Ledol	27.88	0.97	$C_{15}H_{26}O$	222	876	846
β-Cadin-4-en-10-ol	28.53	1.19	$C_{15}H_{26}O$	222	843	793
(Z)-9-octadecenoic acid	30.01	0.55	$C_{18}H_{34}O_2$	282	777	763
Arachidonic acid methyl ester	30.94	1.98	$C_{21}H_{34}O_2$	318	844	786
2-Methylenecholestan-3-ol	31.68	3.35	$C_{28}H_{48}O$	400	818	765
1-Heptatriacotanol	32.11	2.77	$C_{37}H_{76}O$	536	826	805

R.T.: Retention time.

Table 5. Chemical composition of the EOs from *V. agnus-castus* fruits.

Compound Name	R.T.(min)	Area %	Molecular Formula	Molecular Weight	Standard Index	Reverse Standard Index
α-Pinene	6.18	2.58	$C_{10}H_{16}$	136	911	913
β-Thujene	7.43	1.32	$C_{10}H_{16}$	136	899	901
Eucalyptol	9.51	16.65	$C_{10}H_{18}O$	154	928	930
cis-Caryophyllene	20.26	3.73	$C_{15}H_{24}$	204	906	907
γ-Elemene	22.74	41.59	$C_{15}H_{24}$	204	876	880
Caryophyllene oxide	25.09	2.55	$C_{15}H_{24}O$	220	773	787
Preg-4-en-3-one,17α-hydroxy-17β-cyano-	27.74	0.82	$C_{20}H_{27}NO_2$	313	744	750
Geranyllinalool	29.79	17.98	$C_{20}H_{34}O$	290	831	835
(Nerolidyl acetate)	30.36	11.63	$C_{17}H_{28}O_2$	264	742	743
Nerolidol	31.53	1.16	$C_{15}H_{26}O$	222	784	813

R.T.: Retention time.

3.5. Antifungal Activity of the Model Linen Treated with V. agnus-castus Leaf EO

The antifungal activity of the studied EOs illustrates that the leaf EO from *V. agnus-castus* has the highest and best activity against the three fungi. The samples of the linen fibers were incubated with each fungus in petri dishes containing concentrated oil (Figure 4).

The results of the antifungal activity after the application of *V. agnus-castus* leaf EO as a fumigant agent to the model linen fibers similar to those used for the mummy are shown in Table 6. The lowest concentrations of EO from the *V. agnus-castus* leaf when the linen pieces were fumigated caused a 100% growth inhibition of the three fungi (1000 µL/mL, 500 µL/mL, and 500 µL/mL for *A. flavus*, *C. cladosporioides* and *P. chrysogenum*, respectively).

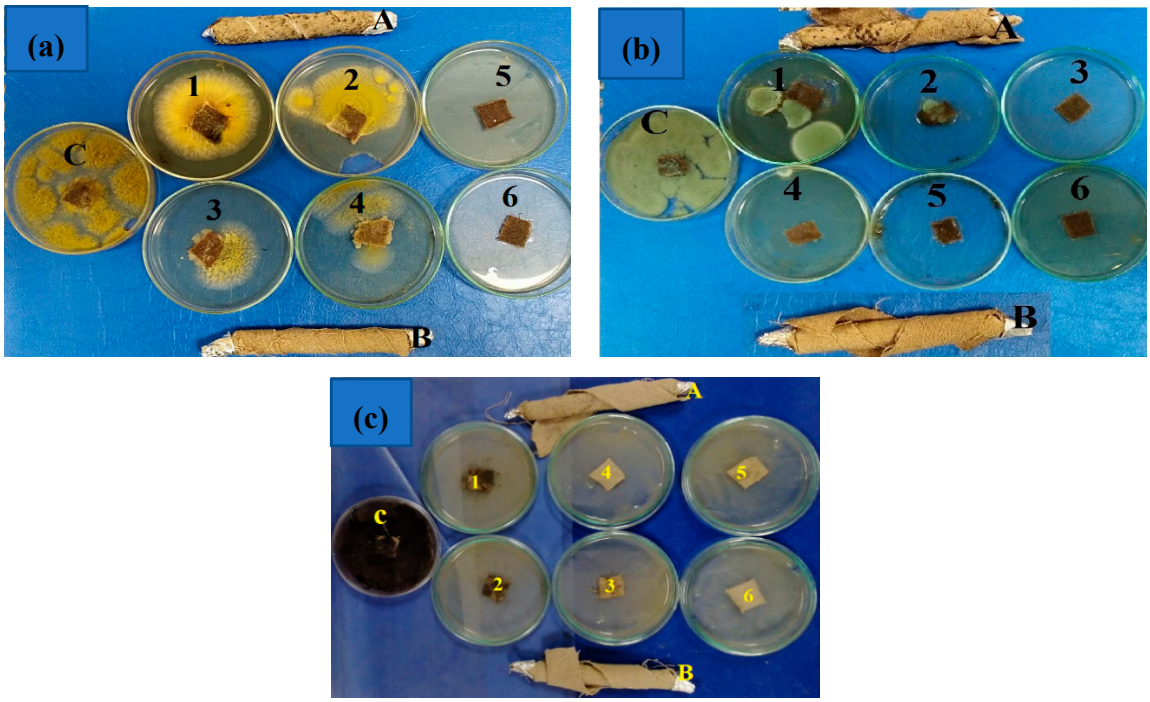

Figure 4. Photo of the antifungal activity of linen fumigated with different concentrations of *V. agnus-castus* leaf essential oil against (**a**) *Aspergillus flavus*, (**b**) *Penicillium chrysogenum*, and (**c**) *C. cladosporioides*. A: Linen infected with the fungus; B: linen treated with the oil; C: control treatment

Table 6. Antifungal activity of the fumigated model linen fibers with *V. agnus-castus* leaf essential oil.

Oil Concentration (µL/mL)	Growth Inhibition (%)		
	A. flavus	*C. cladosporioides*	*P. chrysogenum*
0 (control)	0.00 ^{e}	0.00 ^{d}	0.00 ^{d}
125	9.25 ± 3.2 ^{d}	75.92 ± 3.21 ^{c}	29.63 ± 3.2 ^{c}
250	38.88 ± 5.55 ^{c}	78.14 ± 0.64 ^{b}	92.59 ± 3.21 ^{b}
500	72.22 ± 5.55 ^{b}	100 ^{a}	100 ^{a}
750	75.92 ± 3.21 ^{b}	100 ^{a}	100 ^{a}
1000	100 ^{a}	100 ^{a}	100 ^{a}
2000	100 ^{a}	100 ^{a}	100 ^{a}

Means with the same letter within the same column are significantly difference according to the Least Significant Difference (LSD 0.05).

3.6. SEM Examination

The model linen pieces treated with the lowest concentrations of the *V. agnus-castus* leaf EO caused 100% inhibition to the growth of fungi and, to compare them with the control treatment, were subjected to SEM examination. Figure 5a–d shows the SEM images with different magnifications of the linen fibers after treatment with EO without fungi. These photos show the distribution of the *V. agnus-castus* leaf EO spots over the fibers. As shown in Figure 5i,j, the linen fibers not treated with the EOs feature significant growth of fungal mycelium from *A. flavus* (e,f), *C. cladosporioides* (g,h), and *P. chrysogenum* (i,j).

Figure 6 shows the SEM images of the linen fibers treated with *V. agnus-castus* leaf EO and inoculated with fungi. SEM examination showed the morphological changes in the hyphae. The linen fibers treated with *V. agnus-castus* leaf EO showed clear damage in the fungus, which is evident in changing the form of the hyphae and the absorption and split in other cases (a,b). In the control group, the hyphae were round and full with a smooth surface (Figure 5e–j), while, like the colonized linen

fibers treated with *V. agnus-castus* leaf EO, the structures of the hyphae of the fungi were damaged (Figure 6a–f), deformed, and had rough surfaces.

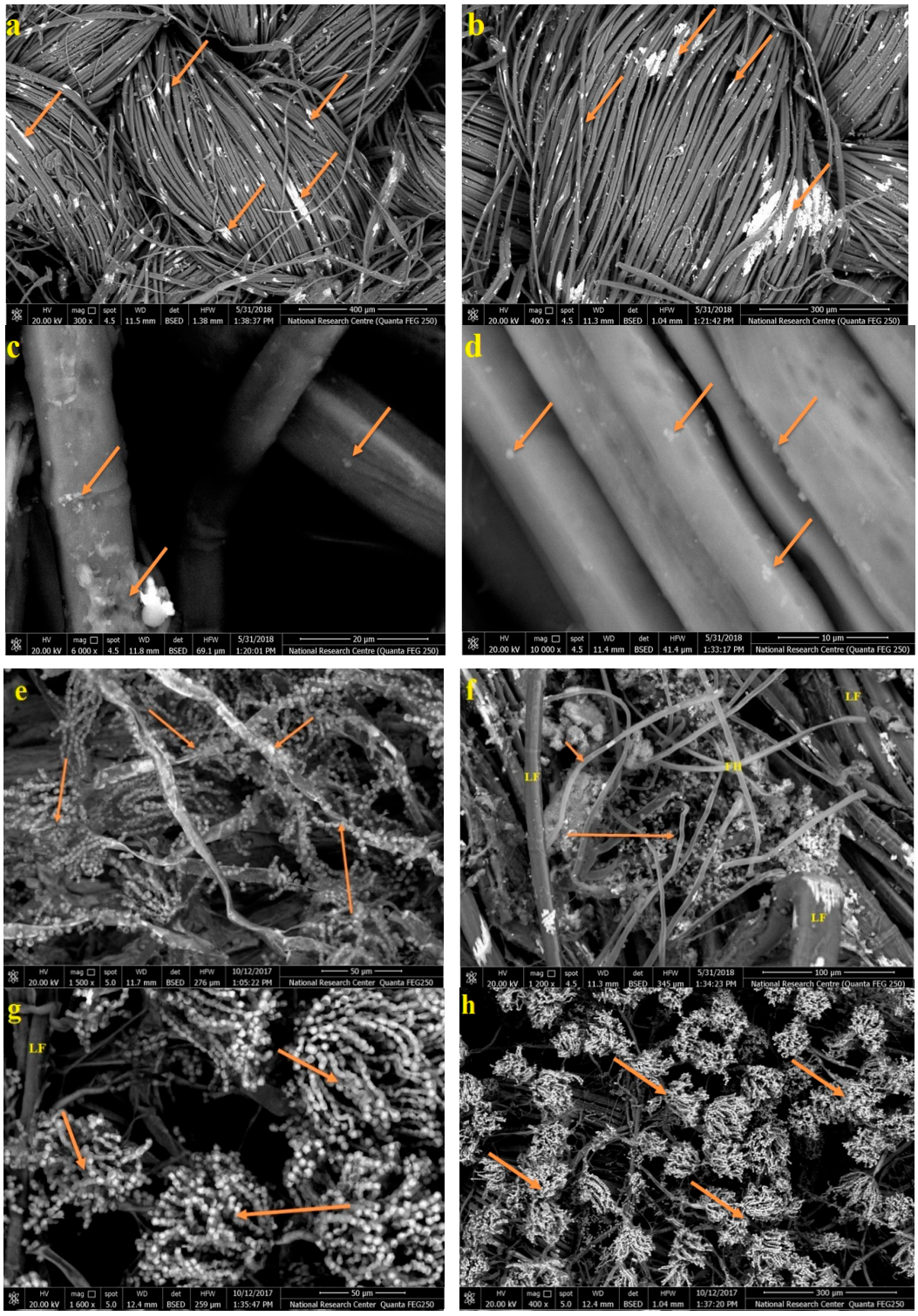

Figure 5. *Cont.*

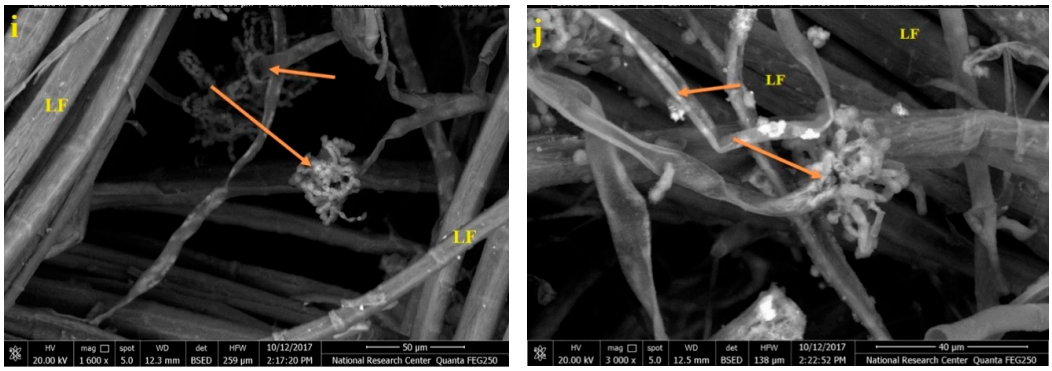

Figure 5. SEM images of the linen fibers treated with *V. agnus-castus* leaf oil (**a**–**d**); linen fibers colonized with *A. flavus* (**e**,**f**), *C. cladosporioides* (**g**,**h**), and *P. chrysogenum* (**i**,**j**). LF: Linen fiber; arrows refer to the growth of the fungi hayphae.

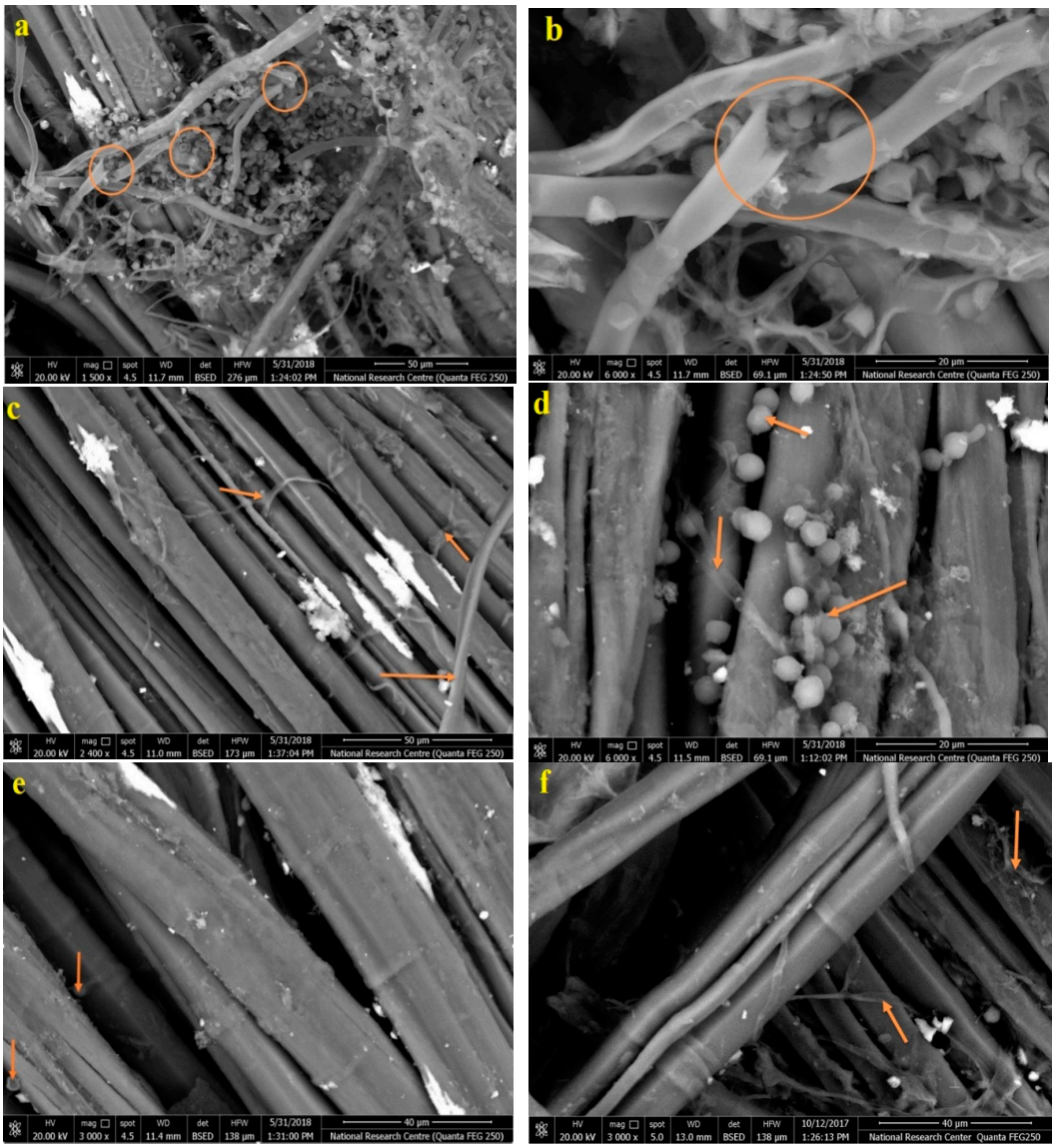

Figure 6. SEM images of the linen fibres treated with the oil and colonized with the fungi; (**a**,**b**) linen treated with oil and incubated with *A. flavus;* (**c**,**d**) linen treated with oil and incubated with *C. cladosporioides;* (**e**,**f**) linen treated with oil and incubated with *P. chrysogenum*. Arrows and circles refer to the growth and damage found in the fungal structures.

Previous studies have indicated the significant growth of fungal mycelium. Pulp paper from Whatman, cotton, or chemical pulp showed deterioration symptoms when inoculated with *Trichoderma harzianum* and *Paecilomyces variotii* [70]. Papyrus strips treated with some additives decreased the growth of *A. flavus*, *A. niger*, and *C. gloeosporioides* compared to the control treatment [10]. An erosion of fiber morphology occurred in Linen pulp fibers when inoculated with *A. niger* [11], but with the addition of some plant source additives, this growth decreased.

Finally, according to the SEM examination of linen fibres treated with EO and inoculated with the fungi, the *V. agnus-castus* leaf EO inhibited the growth of mycelium and was able to effectively destroy the morphology and the structure of the hyphae. This study suggests a novel eco-friendly treatment of model linen fibers similar to the method used in the ancient Egyptian mummification of the child mummy using the essential oil of *V. agnus-castus* leaf. This oil offered potent activity against the growth of *A. flavus*, *C. cladosporioides*, and *P. chrysogenum*, which were previously isolated from the child mummy and inoculated into the designed model linen fiber for mummification.

4. Conclusions

Isolated fungi *A. flavus*, *C. cladosporioides*, and *P. chrysogenum* from an ancient Egyptian mummy were examined for their roles as biodetergent agents in the linen fibres that were used. The analytical methods of FTIR and XRD showed that these three fungi affected the chemical composition of the linen samples through changes in the wavenumbers of the functional groups of the main chemical structures of the standard, original, and linen fibers infected with fungi. Five EOs extracted from *E. africanus* leaf, *V. agnus-castus* leaf and fruit, *C. citratus* leaf, and *R. officinalis* leaf were tested for their antifungal activity. *V. agnus-castus* leaf oil produced the best inhibition of fungal mycelial growth. The effectiveness of the innovated and treated model linen fibers with *V. agnus-castus* leaf EO was achieved, and SEM examination showed inhibited growth of the fungal mycelium, as well as changes in the morphology and structure of the hyphae.

Author Contributions: M.M.A.M., M.E.-H., M.Z.M.S. and H.M.A. designed the experiments, conducted the laboratory analyses, wrote parts of the manuscript, and interpreted the results; all co-authors contributed in writing and revising the article. All authors have read and agreed to the published version of the manuscript.

Funding: This research was funded by Researchers Supporting Project number (RSP-2019/123), King Saud University, Riyadh, Saudi Arabia.

Acknowledgments: Researchers Supporting Project number (RSP-2019/123) King Saud University, Riyadh, Saudi Arabia.

Conflicts of Interest: The authors declare no conflicts of interest.

References

1. Salem, M.Z.M.; Zidan, Y.E.; Mansour, M.M.A.; El Hadidi, N.M.N.; Abo Elgat, W.A.A. Antifungal activities of two essential oils used in the treatment of three commercial woods deteriorated by five common mold fungi. *Inter. Biodeterior. Biodegrad.* **2016**, *106*, 88–96. [CrossRef]
2. Ashmawy, N.A.; Al Farraj, D.A.; Salem, M.Z.M.; Elshikh, M.S.; Al-Kufaidy, R.; Alshammari, M.k.; Salem, A.Z.M. Potential impacts of *Pinus halepensis* Miller trees as a source of phytochemical compounds: Antibacterial activity of the cones essential oil and n-butanol extract. *Agrofores. Syst.* **2018**. [CrossRef]
3. Al-Huqail, A.A.; Behiry, S.I.; Salem, M.Z.M.; Ali, H.M.; Siddiqui, M.H.; Salem, A.Z.M. Antifungal, antibacterial, and antioxidant activities of *Acacia saligna* (Labill.) H. L. Wendl. flower extract: HPLC analysis of phenolic and flavonoid compounds. *Molecules* **2019**, *24*, 700. [CrossRef] [PubMed]
4. Behiry, S.I.; Okla, M.K.; Alamri, S.A.; EL-Hefny, M.; Salem, M.Z.M.; Alaraidh, I.A.; Ali, H.M.; Al-Ghtani, S.M.; Monroy, J.C.; Salem, A.Z.M. Antifungal and antibacterial activities of *Musa paradisiaca* L. peel extract: HPLC analysis of phenolic and flavonoid contents. *Processes* **2019**, *7*, 215. [CrossRef]
5. Behiry, S.I.; EL-Hefny, M.; Salem, M.Z.M. Toxicity effects of *Eriocephalus africanus* L. leaf essential oil against some molecularly identified phytopathogenic bacterial strains. *Nat. Prod. Res.* **2019**. [CrossRef]

6. Hamad, Y.K.; Abobakr, Y.; Salem, M.Z.M.; Ali, H.M.; Al-Sarar, A.S.; Al-Zabib, A.A. Activity of plant extracts/essential oils against some plant pathogenic fungi and mosquitoes: GC/MS analysis of bioactive compounds. *BioResources* **2019**, *14*, 4489–4511. [CrossRef]
7. Mohamed, W.A.; Mansour, M.M.A.; Salem, M.Z.M. *Lemna gibba* and *Eichhornia crassipes* extracts: Clean alternatives for deacidification, antioxidation and fungicidal treatment of historical paper. *J. Clean. Prod.* **2019**, *219*, 846–855. [CrossRef]
8. Okla, M.K.; Alamri, S.A.; Salem, M.Z.M.; Ali, H.M.; Behiry, S.I.; Nasser, R.A.; Alaraidh, I.A.; Al-Ghtani, S.M.; Soufan, W. Yield, phytochemical constituents, and antibacterial activity of essential oils from the leaves/twigs, branches, branch wood, and branch bark of Sour Orange (*Citrus aurantium* L.). *Processes* **2019**, *7*, 363. [CrossRef]
9. Salem, M.Z.M.; Behiry, S.I.; EL-Hefny, M. Inhibition of *Fusarium culmorum, Penicillium chrysogenum* and *Rhizoctonia solani* by n-hexane extracts of three plant species as a wood-treated oil fungicide. *J. Appl. Microbiol.* **2019**, *126*, 1683–1699. [CrossRef]
10. Taha, A.S.; Salem, M.Z.M.; Abo Elgat, W.A.A.; Ali, H.M.; Hatamleh, A.A.; Abdel-Salam, E.M. Assessment of the impact of different treatments on technological and antifungal properties of produced Papyrus (*Cyperus papyrus* L.) sheets. *Materials* **2019**, *12*, 620. [CrossRef]
11. Taha, A.S.; Abo Elgat, W.A.A.; Salem, M.Z.M.; Ali, H.M.; Fares, Y.G.E.; Elshikh, M.S. Impact of some plant source additives on enhancing the properties and antifungal activities of pulp made from Linen fibers. *BioResources* **2019**, *14*, 6025–6046.
12. Tajidin, N.E.; Ahmad, S.H.; Rosenani, A.B.; Azimah, H.; Munirah, M. Chemical composition and citral content in lemongrass (*Cymbopogon citratus*) essential oil at three maturity stages. *Afri. J. Biotechnol.* **2012**, *11*, 2685–2693. [CrossRef]
13. Pengelly, A. *The Constituents of Medicinal Plants (Eds): An Introduction to the Chemistry and Therapeutics of Herbal Medicine*; CABI Publishing: England, UK, 2004; pp. 85–103.
14. de Silva, B.C.; Guterres, S.S.; Weisheimer, V.; Schapoval, E.E.S. Antifungal activity of the lemongrass oil and citral against Candida species. *Braz. J. Infect. Dis.* **2008**, *12*, 63–66. [CrossRef] [PubMed]
15. Schaneberg, B.T.; Khan, I.A. Comparison of extraction methods for marker compounds in the essential oil of lemongrass by GC. *J. Agric. Food Chem.* **2002**, *50*, 1345–1349. [CrossRef]
16. Daferera, D.J.; Ziogas, B.N.; Polissiou, M.G. The effectiveness of plant essential oils on the growth of *Botrytis cinerea*, *Fusarium* sp. and *Clavibacter michiganensis* sub sp. michiganensis. *Crop. Prot.* **2003**, *22*, 39–44. [CrossRef]
17. Naik, M.I.; Fomda, B.A.; Jaykumar, E.; Bhat, J.A. Antibacterial activity of lemongrass (*Cymbopogon citratus*) oil against some selected pathogenic bacteria. *Asian Pac. J. Trop. Med.* **2010**, *3*, 535–538. [CrossRef]
18. Domokos, J.; Hethelyi, E.; Palinkas, J.; Szirmai, S.; Tulok, M.H. Essential oil of rosemary (*Rosmarinus officinalis* L.) of Hungarian origin. *J. Essent. Oil Res.* **1997**, *9*, 41–45. [CrossRef]
19. Salido, S.; Altarejos, J.; Nogueras, M.; Sanchez, A.; Lugue, P. Chemical composition and seasonal variations of rosemary oil from southern Spain. *J. Essen. Oil Res.* **2003**, *15*, 10–14. [CrossRef]
20. Hendel, N.; Larous, L.; Belbey, L. Antioxidant activity of rosemary (*Rosmarinus officinalis* L.) and its in vitro inhibitory effect on *Penicillium digitatum*. *Int. Food Res. J.* **2016**, *23*, 1725–1732.
21. Stojković, D.; Soković, M.; Glamočlija, J.; Džamić, A.; Ćirić, A.; Ristić, M.; Grubišić, D. Chemical composition and antimicrobial activity of Vitex agnus-castus L. fruits and leaves essential oils. *Food Chem.* **2011**, *128*, 1017–1022. [CrossRef]
22. Merle, H.; Verdeguer, M.; Blazquez, M.A.; Boira, H. Chemical composition of the essential oils from Eriocephalus africanus L. var. africanus populations growing in Spain. *Flavour Fragr. J.* **2007**, *22*, 461–464. [CrossRef]
23. Salie, F.; Eagles, P.F.; Leng, H.M. Preliminary antimicrobial screening of four South African Asteraceae species. *J. Ethnopharmacol.* **1996**, *52*, 27–33. [CrossRef]
24. Górny, R.L.; Reponen, T.; Willeke, K.; Schmechel, D.; Robine, E.; Boissier, M.; Grinshpun, S.A. Fungal fragments as indoor air biocontaminants. *Appl. Environ. Microbiol.* **2002**, *68*, 3522–3531. [CrossRef] [PubMed]
25. Piñar, G.; Piombino-Mascali, D.; Maixner, F.; Zink, A.; Sterflinger, K. Microbial survey of the mummies from the Capuchin Catacombs of Palermo, Italy: Biodeterioration risk and contamination of the indoor air. *FEMS Microbiol. Ecol.* **2013**, *86*, 341–356. [CrossRef] [PubMed]

26. Geweely, N.S.; Afifi, H.A.; Ibrahim, D.M.; Soliman, M.M. Efficacy of essential oils on fungi isolated from archaeological objects in Saqqara excavation, Egypt. *Geomicrobiol. J.* **2019**, *36*, 148–168. [CrossRef]
27. Allsopp, D.E. Worldwide wastage: The economics of biodeterioration. *Microbiol. Tod.* **2011**, *38*, 150–153.
28. Kavkler, K.; Gunde-Cimerman, N.; Zalar, P.; Demsar, A. Fungal contamination of textile objects preserved in Slovene museums and religious institutions. *Int. Biodeterior. Biodegrad.* **2015**, *97*, 51–59. [CrossRef]
29. Sterflinger, K. Fungi: Their role in deterioration of cultural heritage. *Fungal Biol. Rev.* **2010**, *24*, 47–55. [CrossRef]
30. Montegut, D.; Indictor, N.; Koestler, R. Fungal deterioration of cellulosic textiles: A review. *Int. Biodeterior.* **1991**, *28*, 209–226. [CrossRef]
31. Sequeira, S.; Cabrita, E.J.; Macedo, M.F. Antifungals on paper conservation: An overview. *Int. Biodeterior. Biodegrad.* **2012**, *74*, 67–86. [CrossRef]
32. Gutarowska, B.; Pietrzak, K.; Machnowski, W.; Milczarek, J.M. Historical textiles – a review of microbial deterioration analysis and disinfection methods. *Tex. Res. J.* **2017**, *87*, 2388–2406. [CrossRef]
33. Montanari, M.; Melloni, V.; Pinzari, F.; Innocenti, G. Fungal biodeterioration of historical library materials stored in Compactus movable shelves. November 2012. *Int. Biodeterior. Biodegrad.* **2012**, *75*, 83–88. [CrossRef]
34. Lech, T.; Ziembinska-Buczynska, A.; Krupa, N. Analysis of microflora present on historical textiles with the use of molecular techniques. *Int. J. Conserv. Sci.* **2015**, *6*, 137–144.
35. Čavka, M.; Glasnović, A.; Janković, I.; Sikanjić, P.; Perić, B.; Brkljacić, B.; Mlinarić-Missoni, E.; Skrlin, J. Microbiological analysis of a mummy from the archeological museum in Zagreb. *Coll. Antropol.* **2010**, *34*, 803–805. [PubMed]
36. Mansour, M. Impact of storage conditions on biodeterioration of ancient Egyptian child mummies by xerophilic fungi. *Egy. J. Archaeol. Restorat. Stud.* **2018**, *8*, 97–107.
37. Miller, A.; Laiz, L.; Dionísio, A.; Macedo, M.; Saiz-Jimenez, C. Growth of phototrophic biofilms from limestone monuments under laboratory conditions. *Int. Biodeterior. Biodegr.* **2009**, *63*, 860–867. [CrossRef]
38. Segal, L.; Creely, J.J.; Martin, A.E., Jr.; Conrad, C.M. An empirical method for estimating the degree of crystallinity of native cellulose using the X-ray diffraction. *Tex. Res. J.* **1959**, *29*, 786–794. [CrossRef]
39. Salem, M.Z.M.; Ali, H.M.; El-Shanhorey, N.A.; Abdel-Megeed, A. Evaluation of extracts and essential oil from *Callistemon viminalis* leaves: Antibacterial and antioxidant activities, total phenolic and flavonoid contents. *Asian Pac. J. Trop. Med.* **2013**, *6*, 785–791. [CrossRef]
40. Hussein, H.S.; Salem, M.Z.M.; Soliman, A.M. Repellent, attractive, and insecticidal effects of essential oils from *Schinus terebinthifolius* fruits and *Corymbia citriodora* leaves on two whitefly species, *Bemisia tabaci* and *Trialeurodes ricini*. *Sci. Hortic.* **2017**, *216*, 111–119. [CrossRef]
41. Wiley/NIST. *The Wiley/NBS Registry of Mass Spectral Data*, 8th ed.; Wiley: New York, NY, USA, 2008.
42. Salem, M.Z.M.; Mansour, M.M.A.; Elansary, H.O. Evaluation of the effect of inner and outer bark extracts of Sugar Maple (*Acer saccharum var. saccharum*) in combination with citric acid against the growth of three common molds. *J. Wood Chem. Technol.* **2019**, *39*, 136–147. [CrossRef]
43. EL-Hefny, M.; Ashmawy, N.A.; Salem, M.Z.M.; Salem, A.Z.M. Antibacterial activity of the phytochemicals-characterized extracts of *Callistemon viminalis, Eucalyptus camaldulensis* and *Conyza dioscoridis* against the growth of some phytopathogenic bacteria. *Microb. Pathog.* **2017**, *113*, 348–356. [CrossRef] [PubMed]
44. Salem, M.Z.M.; Zidan, Y.E.; Mansour, M.M.A.; El Hadidi, N.M.N.; Abo Elgat, W.A.A. Evaluation of usage three natural extracts applied to three commercial wood species against five common molds. *Inter. Biodeterior. Biodegrad.* **2016**, *110*, 206–226. [CrossRef]
45. Salem, M.Z.M.; Mansour, M.M.A.; Mohamed, W.S.; Ali, H.M.; Hatamleh, A.A. Evaluation of the antifungal activity of treated Acacia saligna wood with Paraloid B-72/TiO_2 nanocomposites against the growth of *Alternaria tenuissima*, *Trichoderma harzianum*, and *Fusarium culmorum*. *Bio. Res.* **2017**, *12*, 7615–7627.
46. Lopez, P.; Sanchez, C.; Batlle, R.; Nerin, C. Solid-and vapor-phase antimicrobial activities of six essential oils: Susceptibility of selected foodborne bacterial and fungal strains. *J. Agric. Food Chem.* **2005**, *53*, 6939–6946. [CrossRef]
47. Nedorostova, L.; Kloucek, P.; Kokoska, L.; Stolcova, M.; Pulkrabek, J. Antimicrobial proprieties of selected essential oils in vapour phase against foodborne bacteria. *Food Control.* **2009**, *20*, 157–160. [CrossRef]
48. Zimmermann, B.; Tkalčec, Z.; Mešić, A.; Kohler, A. Characterizing aeroallergens by Infrared Spectroscopy of fungal spores and pollen. *PLoS ONE* **2015**, *10*, e0124240. [CrossRef]

49. Gerd, W.; Margarete, P.; Dietrich, F. Hexafluoropropanol as Valuable Solvent for Lignin in UV and IR Spectroscopy. *Holzforschung* **1983**, *37*, 303–307.
50. Kosa, G.; Kohler, A.; Tafintseva, V.; Zimmermann, B.; Forfang, K.; Afseth, N.K.; Tzimorotas, D.; Vuoristo, K.S.; Horn, S.J.; Mounier, J.; et al. Microtiter plate cultivation of oleaginous fungi and monitoring of lipogenesis by high-throughput FTIR spectroscopy. *Microb. Cell Fact.* **2017**, *16*, 101. [CrossRef]
51. Zhang, Y.L.; Chen, J.; Lei, Y.; Zhou, Q.; Sun, S.; Noda, I. Discrimination of different red wine by Fourier transform infrared and two-dimensional infrared correlation spectroscopy. *J. Mol. Struct.* **2010**, *974*, 144–150. [CrossRef]
52. Herrera, R.; Erdocia, X.; Llano-Ponte, R.; Labidi, J. Characterization of hydrothermally treated wood in relation to changes on its chemical composition and physical properties. *J. Anal. Appl. Pyrol.* **2014**, *107*, 256–266. [CrossRef]
53. Zhou, C.; Jiang, W.; Cheng, Q.; Via, B.K. Multivariate calibration and model integrity for wood chemistry using Fourier transform infrared spectroscopy. *J. Anal. Methods Chem.* **2015**, 1–9. [CrossRef] [PubMed]
54. Gandolfo, D.S.; Mortimer, H.; Woodhall, J.W.; Boonham, N. Fourier transform infra-red spectroscopy using an attenuated total reflection probe to distinguish between Japanese larch, pine and citrus plants in healthy and diseased states. *Spectrochim Acta A* **2016**, *163*, 181–188. [CrossRef] [PubMed]
55. Salem, M.Z.M.; Hamed, S.A.M.; Mansour, M.M.A. Assessment of efficacy and effectiveness of some extracted bio-chemicals as bio-fungicides on Wood. *Drv. Ind.* **2019**, *70*, 337–350. [CrossRef]
56. Hong, Y.; Dashtban, M.; Chen, S.; Song, R.; Qin, W. Lignin in paper mill sludge is degraded by white-rot fungi in submerged fermentation. *J. Microb. Biochem. Technol.* **2015**, *7*, 177–181.
57. Shi, J.; Xing, D.; Lia, J. FTIR Studies of the Changes in Wood Chemistry from Wood Forming Tissue under Inclined Treatment. *Energy Procedia* **2012**, *16*, 758–762. [CrossRef]
58. Mohebby, B. Attenuated total reflection infrared spectroscopy of white-rot decayed beech wood. *Int. Biodeterior. Biodegrad.* **2005**, *55*, 247–251. [CrossRef]
59. Silva-Carvalho, R.; Silva, J.P.; Ferreirinha, P.; Leitão, A.F.; Andrade, F.K.; Gil da Costa, R.M.; Cristelo, C.; Rosa, M.F.; Vilanova, M.; Gama, F.M. Inhalation of Bacterial Cellulose Nanofibrils Triggers an Inflammatory Response and Changes Lung Tissue Morphology of Mice. *Toxicol. Res.* **2019**, *35*, 45–63. [CrossRef]
60. Duarte, E.B.; das Chagas, B.S.; Andrade, F.K.; Brígida, A.I.S.; Borges, M.F.; Muniz, C.R.; Souza Filho, M.D.S.M.; Morais, J.P.S.; Feitosa, J.P.A.; Rosa, M.F. Production of hydroxyapatite-bacterial cellulose nanocomposites from agroindustrial wastes. *Cellulose* **2015**, *22*, 3177–3187. [CrossRef]
61. Warnock, M.; Davis, K.; Wolf, D.; Gbur, E. *Soil Burial Effects on Biodegradation and Properties of Three Cellulosic Fabrics*; University of Arkansas: Fayetteville, AR, USA, 2011.
62. Hussain, A.I.; Anwar, F.; Chatha, S.A.S.; Jabbar, A.; Mahboob, S.; Nigam, P.S. *Rosmarinus officinalis* essential oil: Antiproliferative, antioxidant and antibacterial activities. *Braz. J. Microbiol.* **2010**, *41*, 1070–1078. [CrossRef]
63. Takayama, C.; Meirade-Faria, F.; Almeida, A.C.A.; Dunder, R.J.; Manzo, L.P.; Socca, E.A.R.; Batista, L.M.; Salvador, M.J.; Souza-Brito, A.R.M.; Luiz-Ferreira, A. Chemical composition of *Rosmarinus officinalis* essential oil and antioxidant action against gastric damage induced by absolute ethanol in the rat. *Asian Pac. J. Trop. Biomed.* **2016**, *6*, 677–681. [CrossRef]
64. Zaouali, Y.; Bouzaine, T.; Boussaid, M. Essential oils composition in two *Rosmarinus officinalis* L. varieties and incidence for antimicrobial and antioxidant activities. *Food Chem Toxicol.* **2010**, *48*, 3144–3152. [CrossRef] [PubMed]
65. Zoghbi, M.G.B.; Andrade, E.H.; Maia, J.G.S. The essential oil of *Vitex agnus-castus* L. growing in the Amazon region. *Flav. Frag. J.* **1999**, *14*, 211–213. [CrossRef]
66. Asdadi, A.; Hamdouch, A.; Oukacha, A.; Moutaj, R.; Gharby, S.; Harhar, H.; El Hadek, M.; Chebli, B.; Idrissi-Hassani, L.M. Study on chemical analysis, antioxidant and in vitro antifungal activities of essential oil from wild *Vitex agnus-castus* L. seeds growing in area of Argan tree of Morocco against clinical strains of Candida responsible for nosocomial infections. *J. Mycol. Med.* **2015**, *25*, e118–e127. [PubMed]
67. Gonçalves, R.; Vanessa, F.; Ayres, S.; Carlos, E.; Carvalho, M.G.M.; Souza, A.C.; Guimarães, G.M.; Corrêa, C.H.G.; Martins, R.T.; Eliane, O.S.; et al. Chemical composition and antibacterial activity of the essential oil of *Vitex agnus-castus* L. (Lamiaceae). *An. Da Acad. Bras. De Ciências* **2017**, *89*, 2825–2832.
68. Yilar, M.; Bayan, Y.; Onaran, A. Chemical composition and antifungal effects of *Vitex agnus-castus* L. and *Myrtus communis* L. Plants. *Not. Bot. Horti. Agrobo.* **2016**, *44*, 466–471. [CrossRef]

69. Badawy, M.E.I.; Abdelgaleil, S.A.M. Composition and antimicrobial activity of essential oils isolated from Egyptian plants against plant pathogenic bacteria and fungi. *Ind Crop. Prod.* **2014**, *52*, 776–782. [CrossRef]
70. Hassan, R.R.A.; Mansour, M.M.A. A microscopic study of paper decayed by *Trichoderma harzianum* and *Paecilomyces variotii*. *J. Polym. Environ.* **2018**, *26*, 2698–2707. [CrossRef]